chemosensors

MDPI

Article

Capacitive Humidity Sensor with a Rapid Response Time on a GO-Doped P(VDF-TrFE)/LiCl Composite for Noncontact Sensing Applications

Enkhzaya Ganbold [1,2,3], Parshant Kumar Sharma [1,2,3], Eun-Seong Kim [4,*], Do-Nam Lee [5,*] and Nam-Young Kim [1,6,*]

[1] RFIC Bio Centre, Department of Electronics Engineering, Kwangwoon University, 20 Kwangwoon-ro, Nowon-Gu, Seoul 01897, Republic of Korea
[2] Department of Electronics Engineering, Kwangwoon University, 20 Kwangwoon-ro, Nowon-Gu, Seoul 01897, Republic of Korea
[3] NDAC Centre, Kwangwoon University, 20 Kwangwoon-ro, Nowon-Gu, Seoul 01897, Republic of Korea
[4] Wavepia Co., Ltd., Hwanseong-si, Seoul 18469, Republic of Korea
[5] Ingenium College of Liberal Arts (Chemistry), Kwangwoon University, 20 Kwangwoon-ro, Nowon-Gu, Seoul 01897, Republic of Korea
[6] Department of Molecular Medicine and Biopharmaceutical Sciences, Graduate School of Convergence Science and Technology, Seoul National University, Seoul 08826, Republic of Korea
* Correspondence: esk@kw.ac.kr (E.-S.K.); donamlee2@kw.ac.kr (D.-N.L.); nykim@kw.ac.kr (N.-Y.K.)

Abstract: Humidity-sensing devices are widely utilized in various fields, including the environment, industries, food processing, agriculture, and medical processes. In the past few years, the development of noncontact sensors based on moisture detection has increased rapidly due to the COVID-19 pandemic. Moisture-detection, noncontact and breath-monitoring sensors have promising applications in various fields. In this study, we proposed a rapid-response graphene oxide (GO)-doped P(VDF-TrFE)/LiCl nanocomposite-based moisture sensor fabricated on an interdigitated electrode. The synthesis of GO/P(VDF-TrFE)/LiCl resulted in a porous structure with nano-sized holes due to the effect of LiCl. Moreover, doped GO improved the conductivity of the sensing film. The created nanoporous structure improved the recovery time better than the response time, with the times being 4.8 s and 7.8 s, respectively. Not only did our sensor exhibit rapid response and recovery times, it also exhibited a high sensitivity of 1708.8 pF/%RH at 25% to 93%RH. We also presented a real-time breath-monitoring system for noncontact sensing applications based on GO-doped P(VDF-TrFE)/LiCl composites. The results revealed that GO-doped P(VDF-TrFE)/LiCl is a good candidate for fabricating real-time moisture-detection noncontact sensing devices.

Keywords: polymeric composite; graphene oxide; capacitive humidity sensor; breath monitoring; noncontact sensing

Citation: Ganbold, E.; Sharma, P.K.; Kim, E.-S.; Lee, D.-N.; Kim, N.-Y. Capacitive Humidity Sensor with a Rapid Response Time on a GO-Doped P(VDF-TrFE)/LiCl Composite for Noncontact Sensing Applications. *Chemosensors* **2023**, *11*, 122. https://doi.org/10.3390/chemosensors11020122

Academic Editors: Alexander G. Bannov, Tamara Basova, Alexey Glushenkov and Mahmut Durmuş

Received: 21 December 2022
Revised: 31 January 2023
Accepted: 1 February 2023
Published: 7 February 2023

1. Introduction

Controlling various environmental parameters, such as humidity, temperature and pressure, is important in daily life. Among these parameters, relative humidity control still plays an important role in various fields, including agriculture, manufacturing, food processing and biomedical engineering. Recently, humidity sensors have received considerable attention in breath-monitoring and noncontact sensing applications. Water vapor is the dominant component (6%) in inhaled air; hence, a humidity sensor can be used to monitor the rate and depth of a patient's breathing in real time. Breath is a basic physiological characteristic, and it can be used to evaluate breathing problems such as sleep apnea, asthma, bronchitis, and heart diseases. Moreover, the noncontact humidity sensors are based on the moisture of human skin compared with the contact sensor, which can reduce the transmission of viruses and bacteria to a certain extent. Furthermore, research on respiratory diagnostics and noncontact sensors has received increasing attention since the COVID-19 outbreak [1–9].

The proper selection of sensing materials is the key to developing high-performance humidity sensors with high sensitivity, excellent stability, rapid response, and reliability. Therefore, the selection of sensing material is most significant. Several kinds of materials have been used to manufacture humidity sensors, such as ceramic [10], metal oxide [11], nanotubes [12], polymers [13], and carbon materials [14]. However, the complicated synthesis process, limited detecting range, and high cost of sensing materials are still challenging to overcome. In recent years, polymer-based composites were proposed for various sensing applications owing to their diverse structures, easy processability, stability, controllability, and low cost [15,16]. Among them, ferroelectric and piezoelectric poly(vinylidene fluoride-trifluoroethylene) (P(VDF-TrFE)) has been widely studied and used in various applications owing to its easy fabrication, chemical stability, solution processability, and biological compatibility. P(VDF-TrFE) has the properties of binding to several surfaces among various polymers. Moreover, P(VDF-TrFE) is a copolymer of polyvinylidene fluoride (PVDF) and polytrifluoroethylene (PtrFE), and it can be easily conformed to various kinds of surface owing to its excellent mechanical properties and improved polarizability. However, it has a low sensitivity to humidity sensing due to its hydrophobic properties. The sensitivity of P(VDF-TrFE) to water molecules can be improved by adding ionic salt (LiCl) to a polymer-based solution, which can change a hydrophobic surface to a more hydrophilic one and improve its sensitivity to humidity [17–19]. LiCl, as a strong and excellent electrolyte, is a well-known choice for constructing humidity-sensitive composites. Furthermore, even at low relative humidity levels, a single molecule of LiCl may absorb 1000 times its own mass in water vapor. After LiCl addition, the sensitivity of the composite is significantly improved by the interaction between the ionized LiCl and the absorbed water molecules. Recently, LiCl has been widely used to prepare porous surfaces, as well as to improve the sensitivity of polymers [20–23]. Carbon-based nanomaterials are good candidates in humidity sensors due to their excellent surface chemistry and structure designability. To develop high-performance humidity sensors, two-dimensional (2D) graphene oxide (GO) has been widely used as the composite material to improve electrical properties. GO has advantages, such as high electrical and chemical stability, excellent conductivity to water molecules, and high control of functionalization. Additionally, GO has hydrophilic and electrically insulating properties due to its oxygen-containing functional groups. These properties make GO potentially useful as a sensing material. Further, GO is more compatible with polymers than pure graphene, and it is a good candidate for chemical sensing applications [24–28].

Various humidity sensors are used to accurately measure relative humidity, including capacitive, resistive, electromagnetic, gravimetric, and optical measurements. Among these, capacitive humidity sensors have the advantages of low power consumption, ease of fabrication, ease of integration with electronic circuits, and effective cost. Moreover, capacitive humidity sensors are based on changes in capacitance values and offer linearity, high sensitivity, and accuracy compared with other types of humidity sensors. Due to their high sensitivity, high conductivity, and ease of fabrication, interdigitated capacitive (IDC) electrodes are suggested as one of the common designs used for fabricating sensing devices. IDC humidity sensors work on the basis of the electrical characteristics of sensing materials and changes in the dielectric constant in electric fields. When the dielectric-layer-coated IDC electrode absorbs water vapor, the dielectric of the sensing film changes and the capacitance value increases. Recently, these sensors have been used in respiration-monitoring and noncontact applications due to their high sensitivity, as well as their rapid response and recovery times [29–33].

The sensitivity, response, and recovery durations of humidity sensors' sensing performances still need to be improved for a variety of real-time applications, despite the fact that there has been a significant advancement in the field. In this study, we demonstrate a facile way to synthesize GO-doped P(VDF-TrFE)/LiCl fabricated on an IDC electrode for humidity detection for the first time. Inorganic salt (LiCl) is used to enhance the sensitivity of P(VDF-TrFE), and GO is used for high conductivity. LiCl dramatically improves the sensitivity of P(VDF-TrFE), and significantly affects the viscosity and surface balance of P(VDF-TrFE). Moreover, GO can improve the electric conductivity of P(VDF-TrFE). After adding LiCl and GO to P(VDF-TrFE), the hydrophobic surface becomes hydrophilic. As a result of GO-doped P(VDF-TrFE)/LiCl-composite material, high humidity sensitivity (1708.8 pF/%RH), response (4.8 s) and recovery time (7.8 s) were obtained at room temperature. Furthermore, the proposed GO-doped P(VDF-TrFE)/LiCl-composite thin-film-based humidity sensor showed high sensitivity and rapid response to real-time noncontact applications, such as breath monitoring and skin moisture detection.

2. Materials and Methods

2.1. Materials

A graphene oxide aqueous solution was supplied by Graphene Supermarket, (New York, NY, USA). Solvene®200/P200 (Poly(vinylidene fluoride-co-trifluoroethylene)), hydrogen peroxide (H_2O_2), sulfuric acid (H_2SO_4), and ethyl alcohol, 99.5% (C_2H_5OH) were purchased from Sigma-Aldrich, (Seoul, Republic of Korea). Lithium chloride (LiCl) was purchased from Samchun Co., Ltd. (Gangnam-gu, Seoul, Republic of Korea) and N, N-dimethylformamide (DMF) was obtained from Duksan Pure Chemicals Co., Ltd. (Gyeonggi-do, Seoul, Republic of Korea). All other chemicals were of analytical grade and were used without further purification.

2.2. Preparation of the GO-Doped P(VDF-TrFE)/LiCl-Based Sensor

Figure 1a illustrates the solution preparation process of the GO-doped P(VDF-TrFE)/LiCl composite on the IDC electrode through the drop-casting method. First, 2.5 wt% concentration of P(VDF-TrFE) was prepared in DMF by magnetic stirring for 6 h at room temperature. Second, LiCl (2 wt%) was added to the prepared solution and magnetically stirred for approximately 2 h. Finally, GO was doped in the P(VDF-TrFE)/LiCl solution with a ratio of 1:1 and stirred for 2 h. Glass-substrate-based Pt/Ti electrodes (IDCs) were used in this study. To design an IDC electrode, 24 fingers with 100 μm widths, 100 μm finger gaps, and 0.3 μm thick, were fabricated onto an Eagle XG glass wafer. The size of the IDC device was 4.1 mm × 7.75 mm [34,35]. To prepare the GO-doped P(VDF-TrFE)/LiCl-composite-based humidity sensor, the IDC electrode was first cleaned with a piranha solution for 15 min at 80 °C. After Piranha cleaning, the GO-doped P(VDF-TrFE)/LiCl-composite solution was coated on the IDC electrode though the drop-casting method with 6 μL. After coating, the sensors were annealed at 80 °C for approximately 30 min. The equivalent circuit of the IDC electrode and interaction of the composite structure is shown in Figure 1b. The detailed structure of the IDC equivalent circuit is included in the Supplementary Materials (Figure S1). When there was no sensing film present, the IDC produced a substrate capacitance called C_{sub}. The capacitance of the sensing film is C_{film}. As the relative humidity increased, LiCl in GO-doped P(VDF-TrFE) was ionized into LI^+ and Cl^-. Ionized LiCl acts as a free conductor on the IDC electrode. In addition, GO is rich in hydroxyl and carbonyl and effectively absorbs water molecules. The real-time measurement process is shown in Figure 1c. As the finger approaches the prepared GO-doped P(VDF-TrFE)/LiCl-composite-based sensor or the volunteer breathes, the capacitance of the sensor changes and a signal is transmitted to the LCR meter. The received signal of the LCR meter is output as data using BenchVue 2020 Update 2.0 software.

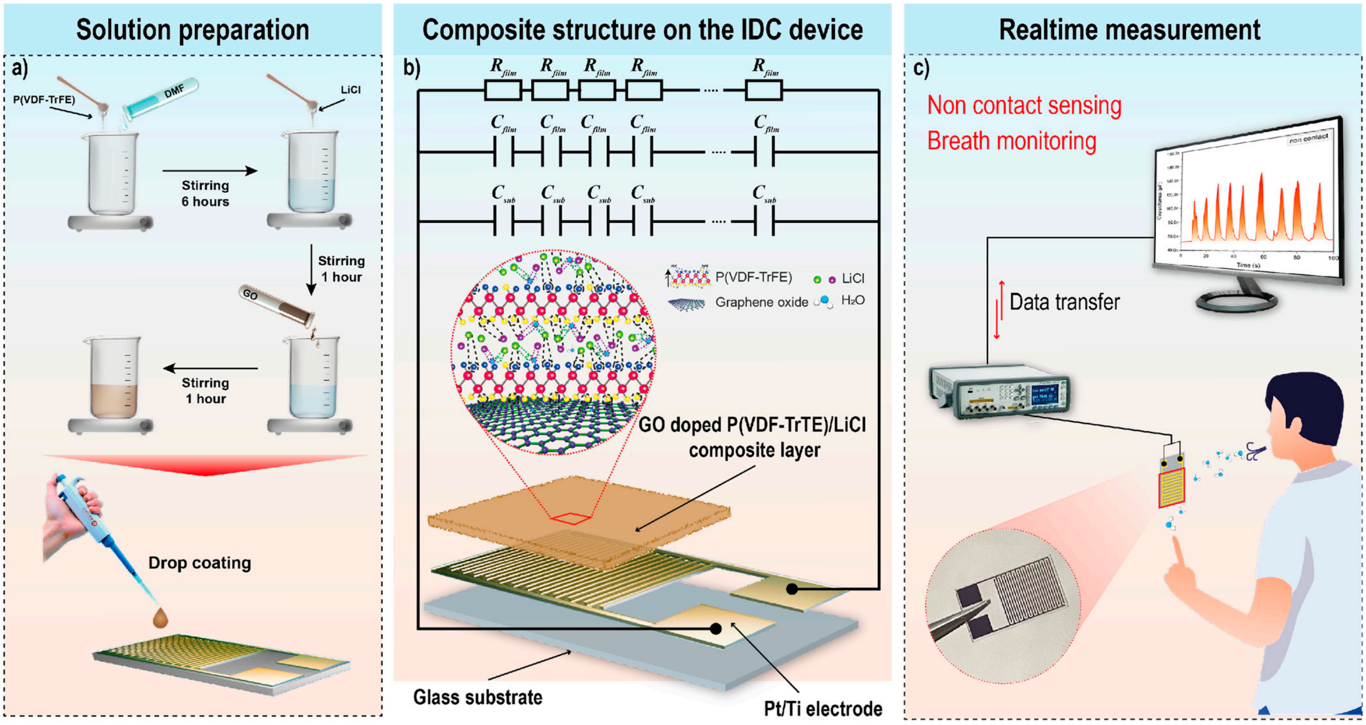

Figure 1. Schematic of the fabrication and measurement processes of a GO-doped P(VDF-TrFE)/LiCl-composite-based humidity sensor. (**a**) Process of solution preparation. (**b**) Equivalent circuit and the composite layer of the prepared GO-doped P(VDF-TrFE)/LiCl-composite-based sensor fabricated on an IDC electrode. (**c**) Real-time measurement of noncontact sensing and breath monitoring.

2.3. Humidity-Sensing Measurement

For humidity-sensing measurements, different RH conditions were achieved by the saturated salt solution method [36]. The GO-doped P(VDF-TrFE)/LiCl nanocomposite sensor was placed at different RH levels at 23 °C. The saturated LiCl, $CaCl_2$, $MgCl_2$, Na_2SO_4, $MgSO_4$, NaCl, KNO_3, and KCI solutions in closed vessels provided 25%, 35%, 46%, 54%, 66%, 75%, 84%, and 93% RH, respectively. The sensors were connected to an LCR meter (Agilent E4980A, Keysight, CA, USA) to record capacitance changes before and after exposing the sample to humidity at a selected frequency of 1 kHz, and the data were transferred to BenchVue software. The relative humidity in the chamber and room was monitored using a hygrometer.

2.4. Sensor Characterization

A field-emission scanning electron microscope (FE-SEM, Quanta 250 FEG, FEI Ltd., Oregon, Seoul, Republic of Korea) was employed to observe the characteristics and porosity of the GO-doped P(VDF-TrFE)/LiCl surfaces. P(VDF-TrFE) and GO-doped P(VDF-TrFE)/LiCl-composite thin films' average roughness and surface morphology were characterized using an atomic force microscope (AFM, XE150, PSIA, Suwon, Republic of Korea). The AFM data were analyzed using the software program XEI (Park Systems Corp., Seoul, Republic of Korea) for obtaining the top and 3D morphological views. To assess the crystallinity and phase transition of the samples with Cu target (wavelength 1.5412 Å) over a 2 range of 10° to 80°, X-ray diffraction (XRD) using a SmartLab diffractometer from Rigaku Corp. (Tokyo, Japan), was used. A Raman spectrometer (LabRam ARAMIS IR2, HORIBA Jobin Yvon SAS Ltd., Jersey, NJ, USA) was used to analyze the combined state of the composite materials and their components of the thin-film surfaces.

3. Results and Discussion

3.1. Characterization of GO-Doped P(VDF-TrFE)/LiCl

The SEM image of the GO-doped P(VDF-TrFE)/LiCl composite is shown in Figure 2a. Without LiCl, the P(VDF-TrFE)-coated humidity sensor was almost completely smooth; however, after the synthesis of LiCl, the surface's morphology changed to that of a sponge-like structure. After adding LiCl, nano- and micro-sized pores formed on the entire surface. The porous structure was preserved even after the synthesis of GO. The nanoholes enhanced the absorption and desorption of water vapor and improved the sensitivity of the GO-doped P(VDF-TrFE)/LiCl-coated IDC electrode. When the surface was enlarged to 2 µm, the size of holes of porosity of GO-doped P(VDF-TrFE)/LiCl was observed to range from nanometers (300 nm) to micrometers (1.1 µm). Figure 2a also shows the cross-section of the GO-doped P(VDF-TrFE)/LiCl-composite film. The thickness of the composite film was ~1.3 um. After adding GO and LiCl, the surface of P(VDF-TrFE) developed a sponge-like structure on the IDC electrode, which had an important effect on relative humidity sensing. SEM images of P(VDF-TrFE) and P(VDF-TrFE)/LiCl composites are included in the Supplementary Materials (Figure S2). The AFM image (80 µm × 80 µm) was employed to characterize the surface morphology and average roughness of the GO-doped P(VDF-TrFE)/LiCl nanocomposite film, as shown in Figure 2b. The root-mean-square (RMS) of the surface roughness was 29.668 nm. The elemental composition of the GO-doped P(VDF-TrFE) was investigated through energy-dispersive X-Ray spectroscopy (EDS), with a magnification level of 5 µm. The investigated results confirmed the presence of C K, F K, Cl K, and O K series, as shown in Figure 2c. The layered EDS image demonstrates the presence of carbon 26.34%, a fluorine series 5.69%, Cl 1.02%, and oxygen 6.65%, respectively, as illustrated in Figure 2c. The EDS mapping confirmed the presence of GO, LiCl, and P(VDF-TrFE) copolymer.

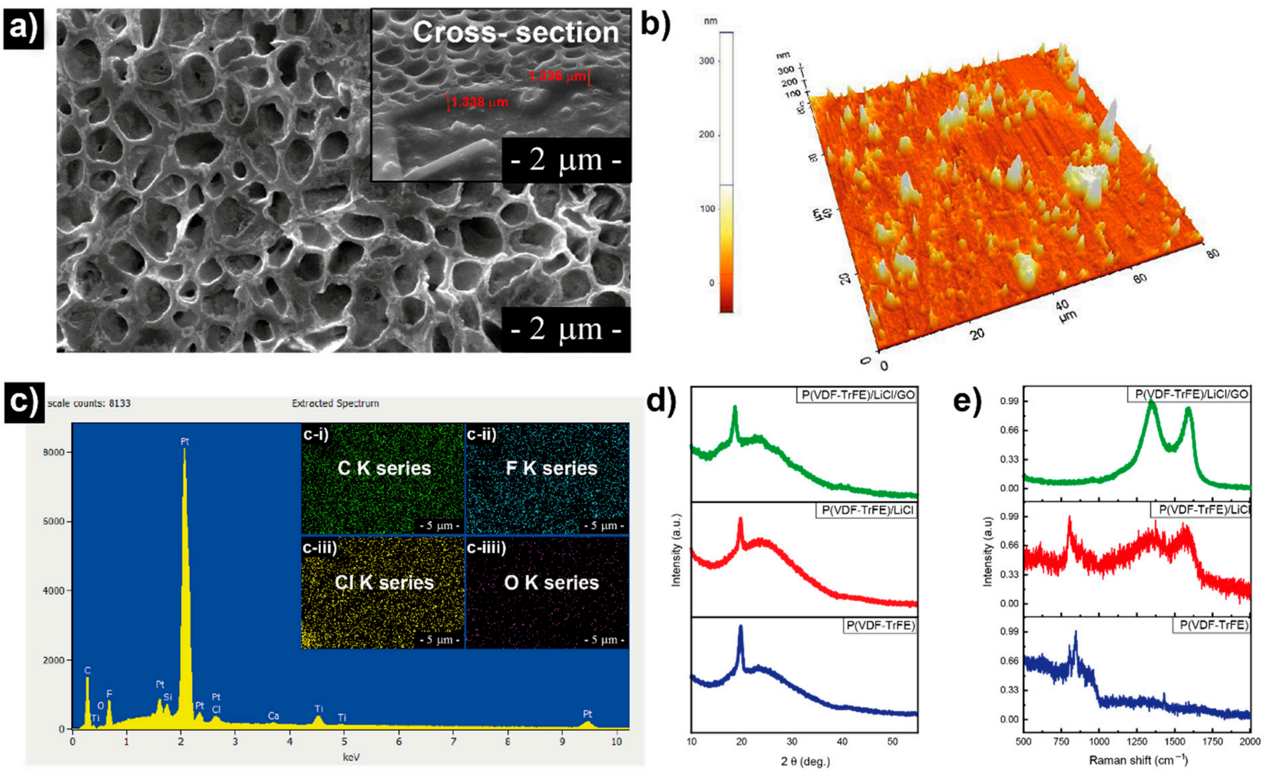

Figure 2. Characterization of the GO-doped P(VDF-TrFE)/LiCl composite based humidity sensor. (**a**) SEM images of the GO-doped P(VDF-TrFE)/LiCl, (**b**) the AFM image composites, (**c**) SEM-EDS analysis and elemental mapping, (**d**) XRD, and (**e**) Raman spectroscopy results of pure P(VDF-TrFE), P(VDF-TrFE)/LiCl, and GO-doped P(VDF-TrFE)/LiCl composites.

XRD analysis was performed to investigate the crystalline structure of P(VDF-TrFE), P(VDF-TrFE)/LiCl, and GO-doped P(VDF-TrFE)/LiCl-composite thin films, shown in Figure 2d. The β-phase peak was obtained from prepared pure P(VDF-TrFE) thin films, and the β-phase of P(VDF-TrFE) was preserved after the synthesis of LiCl and GO. The GO-doped P(VDF-TrFE)/LiCl-composite thin film exhibited a peak at 20°, which was attributed to the (110) orientation planes, which were associated with the polar β-phase. The piezoelectric properties of the semicrystalline polymer, PVDF, and its copolymer P(VDF-TrFE), originate from the crystal structure of their crystalline phases of α, β, γ, and δ. Among the α, β, γ, and δ crystalline phases, the β-phase exhibits the strongest polarization and high piezoelectric, pyro-, and ferro-electricity properties. The crystalline PVDF-TrFE β-phase shows extensive piezoelectric properties, and it has inherent properties of lightweightedness, mechanical flexibility, and easy processing; hence, it is the most preferred. Moreover, the introduction of TrFE into PVDF favors the formation of the ferroelectric β phase in P(VDF-TrFE) and simplifies the fabrication process. The β-phase of P(VDF-TrFE) is very suitable for the development of humidity sensors [37–39]. Raman analysis was conducted to analyze the combined state of the composite material and the components of the thin-film surface. The Raman spectra of pure P(VDF-TrFE), P(VDF-TrFE)/LiCl, and GO-doped P(VDF-TrFE)/LiCl nanocomposites are shown in Figure 2e. As shown in the top graphic of Figure 2e, a sharp Raman peak is observed at 847 cm^{-1} in the spectrum of the P(VDF-TrFE) film on the IDC electrode surface. After adding LiCl, a sharp Raman peak was observed at 805 cm^{-1}. In the bottom graphic of Figure 2e, a shift occurs in the peaks of the GO-doped P(VDF-TrFE)/LiCl nanocomposites observed in the Raman spectrum. For the GO-doped P(VDF-TrFE)/LiCl nanocomposites, the D-band at 1341 cm^{-1} is caused by the defects in the graphene or amorphous carbon, whereas the G-band is observed at 1582 cm^{-1} [40].

3.2. Sensing Properties of the GO-Doped P(VDF-TrFE)/LiCl Composite

The suitable composition of LiCl in the polymer shows excellent humidity-sensing properties. LiCl enhances the porosity and sensitivity of P(VDF-TrFE) due to its hydrophilicity [41]. This is because composite films' electrical conductivity is enhanced by the water molecules that LiCl absorbs. The surface of the sensing film is further altered by the doping of GO in P(VDF-TrFE)/LiCl, which also increases the surface area that can adsorb water molecules and reduces hysteresis during the desorption process. The sensitivity of the GO-doped P(VDF-TrFE)/LiCl was measured using the following equation:

$$S = \frac{(C_{93} - C_{25})}{93 - 25} \tag{1}$$

where C_{90} and C_{30} represent the capacitance values at the highest humidity level (93% RH) and lowest humidity level (25% RH), respectively. Figure 3 shows the humidity performance of the GO-doped P(VDF-TrFE)/LiCl-based humidity sensor with RH levels ranging from 25% to 93% RH. The sensitivity of GO-doped P(VDF-TrFE)/LiCl is shown in Figure 3a. The sensitivity of the GO-doped P(VDF-TrFE)/LiCl nanoporous thin-film-based sensor was 1708.8 pF/%RH. Figure 3b provides information about the linearity of the GO-doped P(VDF-TrFE)/LiCl nanoporous thin film. The GO-doped P(VDF-TrFE)/LiCl nanoporous thin-film-based humidity sensor showed a superior linear relationship (linearity (L): 0.967) in the overall range. The response and recovery times of the GO-doped P(VDF-TrFE)/LiCl-composite-based humidity sensor are shown in Figure 3c. The response and recovery times of the sensor at 30% and 93% RH were 7.8 s and 4.5 s, respectively. Response and recovery time measurement setup is shown in Figure 3d. Moreover, the response and recovery times of P(VDF-TrFE)/LiCl were also measured; however, the results were unstable and the timings were longer than for the GO-doped P(VDF-TrFE)/LiCl. This may be due to the high sensitivity of LiCl to water vapor. The results are shown in Figure S3 of the Supplementary Materials. We investigated the response and recovery times of the prepared humidity sensors using a homemade sensing chamber and an LCR meter (Keysight E4980AL and

BenchVue software) at 23 °C. During the experiment, the prepared sensor was connected to an LCR meter, and the LCR meter recorded the change in sensor capacitance value through the real-time monitoring software BenchVue.

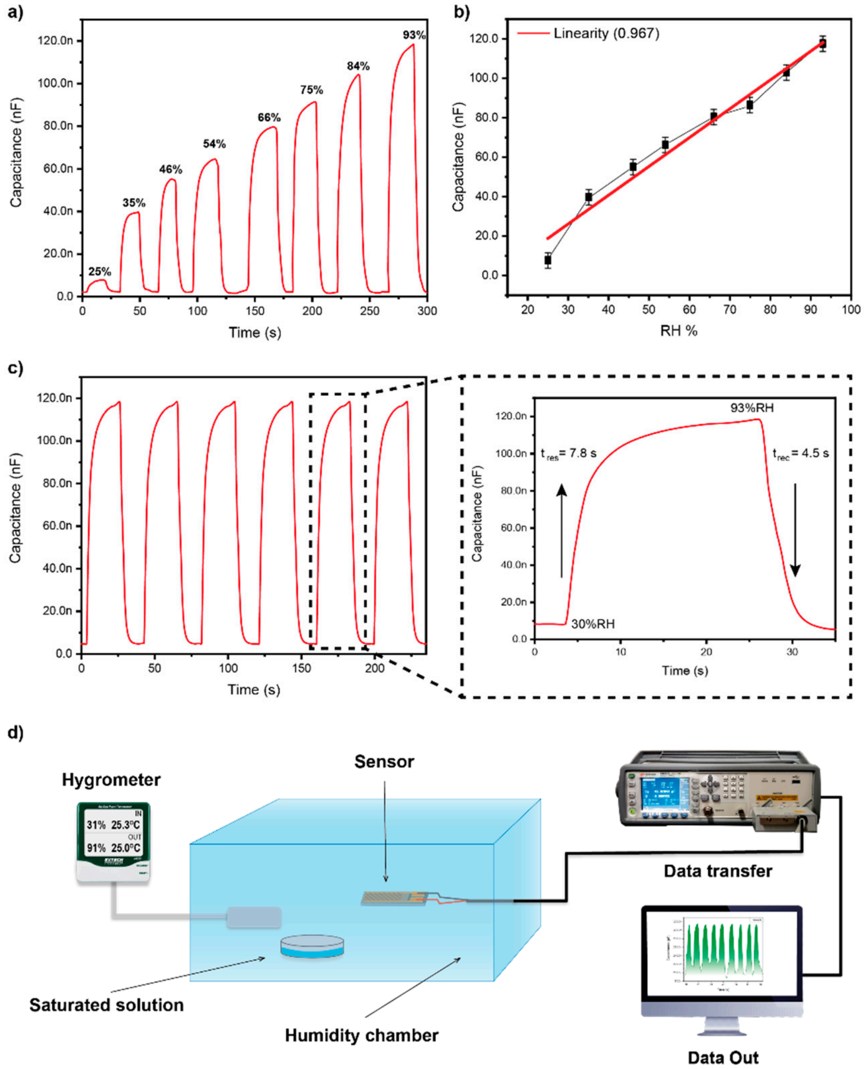

Figure 3. Humidity measurements. (**a**) Sensitivity, (**b**) linearity, (**c**) response and recovery times, and (**d**) measurement setup of response and recovery times.

Moreover, dielectric permittivity and conductivity were measured. The capacitance (C) of the capacitive humidity sensor can be expressed as Equation (2) [42]

$$C = \varepsilon \frac{A}{4k\pi d} \tag{2}$$

where A is the effective area of the two electrodes, ε is the effective dielectric constant of the dielectric layer, k is the electrostatic force constant, and d is the distance between the two electrodes. In our work, dielectric permittivity was measured for sensing thin film. Therefore, it is considered possible to express it by equations at low RH $C_1 = \frac{\varepsilon_1 s}{4k\pi d}$ and high RH $C_2 = \frac{\varepsilon_2 s}{4k\pi d}$. It can also be calculated using the following equation formulated as $C_2 = \frac{\varepsilon_2 s}{4k\pi d}$, where C_1 is capacitance value at low-humidity range and C_2 is capacitance value at high-humidity range. The capacitance value was 2.2 nF at 25% RH range and 118.3 nF at 93% RH range. The ε_1 and ε_2 were calculated as $\frac{C_2}{C_1} = \frac{118.3}{2.2} = \frac{\varepsilon_2}{\varepsilon_1} = 53.77$. Moreover, the compared conductivity data of P(VDF-TrFE), P(VDF-TrFE)/LiCl and GO-doped P(VDF-TrFE) composite sensors are given in Table 1.

Table 1. Conductivity of P(VDF-TrFE)-, P(VDF-TrFE)/LiCl-, and GO-doped P(VDF-TrFE)/LiCl-based humidity sensors.

Sensors	Conductivity (nS)
P(VDF-TrFE)	27.2
P(VDF-TrFE)/LiCl	86.4
GO-doped P(VDF-TrFE)/LiCl	121.3

3.3. Real-Time Monitoring Applications

In this study, we focused on noncontact sensing applications. Recently humidity-based noncontact sensors have been widely studied. Applications of the noncontact-working-principle-based sensor are increasing to improve the comfort of daily life. This is because noncontact sensors are useful in reducing the transmission of viruses and bacteria to a certain extent. During the experiment, P(VDF-TrFE)/LiCl and GO-doped P(VDF-TrFE)/LiCl-composite sensors were placed at the same distance from a human finger. The P(VDF-TrFE)/LiCl-composite sensor did not exhibit noncontact sensing properties, while the GO-doped P(VDF-TrFE)/LiCl exhibited excellent noncontact sensing properties. The capacitance value did not change when the finger was placed close to the P(VDF-TrFE)/LiCl-composite-based humidity sensor connected to the circuit, but the capacitance value was changed when the GO-doped P(VDF-TrFE)/LiCl-composite-based humidity sensor was placed at a distance of about 0.3–0.5 cm. Additionally, the capacitance value remained the same when the sensor was brought closer to a metal object.

We recorded a video to compare the noncontact performance of the P(VDF-TrFE)/LiCl sensor and GO-doped P(VDF-TrFE)/LiCl-composite-based sensorwhich was supporting information (Video S1). The application of noncontact sensors with rapid response is constantly increasing, and noncontact sensors are required to prevent the spread of viral infections by being used to develop uncomplicated applications, such as noncontact buttons for electronic devices. Figure 4a shows a real-time time noncontact sensing experiment process. Capacitance signals were recorded when a human finger approached a sensor device at a distance of 0.3~0.5 cm. We recorded two kinds of data on dry and moist skin. For the moist skin, the capacitance value changed more, as shown in Figure 4b. Figure 4c,d show a noncontact LED that is switched on and off due to finger moisture. Our GO-doped P(VDF-TrFE)/LiCl sensor quickly detected finger moisture without any contact. As the finger approached the sensor, its capacitance was sharply increased due to the fast response to the moisture of the skin, and the LED light was turned on. Moreover, Figure 4e,f show an electric fan turning on and off using the same working principle as with the LED light-on-and-off experiment. As a result, the possibility of developing a noncontact humidity sensor through skin sweat was demonstrated. A circuit design of the noncontact sensing experiment is included in Supplementary Materials (Figure S4).

Respiratory monitoring is useful for medical care, including the treatment of sleep apnea, asthma, bronchitis, heart disease, and lung health. It can aid in the early detection of major respiratory problems. It is possible to use the GO-doped P(VDF-TrFE)/LiCl for real-time breath rate change monitoring. Figure 5a shows the experimental setup created for monitoring human respiration. Using the BenchVue test lab manager software and an LCR meter, sensors were placed within the mask, and sensor capacitance signals were recorded each second when a volunteer inhaled and exhaled. Three types of breath speeds were sequentially evaluated for the volunteer, as shown in Figure 5b. Between exhalation and inhalation during the fast-breathing phase, the capacitance varied by about 217.9–278.1 nF over the course of 14 cycles. The capacitance varied between 182.3 and 336.1 nF in 9 cycles during a normal breathing cycle. The capacitance varied during deep breathing, between 191.8 and 341.5 nF in 14 cycles. These results demonstrate that the nanoporous P(VDF-TrFE)/LiCl structure doped with GO is highly responsive to changes occurring in nose respiration. As illustrated in Figure 5c, breathing control can also be used in apnea instances. The experiment was performed in such a way that the volunteer breathed normally and then purposely stopped breathing. Due to a lack of moisture during an apnea episode, the capacitance value decreased, whereas it increased again after normal breathing. The capacitance signals were recorded without a mask, and the distance between the sensor and the volunteer was 5, 10, 15, or 20 cm, as shown in Figure 5d. A sensing device was connected to the LCR meter, and the signal decreased as the distance increased, as illustrated in Figure 5e. The average capacitance values were 1951 pF, 1633 pF, 1420 pF and 1315 pF at 5, 10, 15 and 20 cm, respectively. Moreover, Figure 5f shows the measured capacitance change in dry diapers exposed to moisture. The capacitance value increased when dry diapers were exposed to moisture. Owing to rapid response and recovery times, our proposed GO-doped P(VDF-TrFE)/LiCl composite fabricated on the IDC electrode can be used in real-time monitoring applications and humidity performances were compared with previous studies, shown in Table 2.

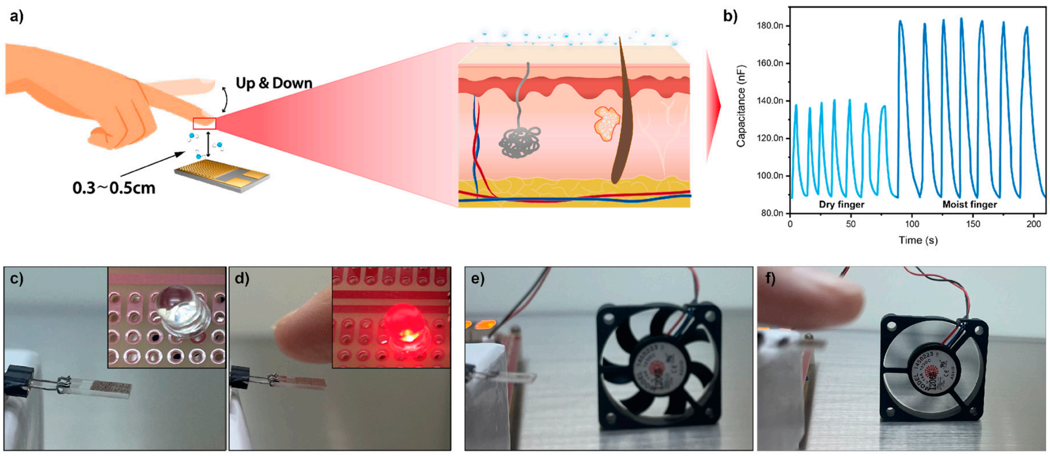

Figure 4. Measurements of the GO-doped P(VDF-TrFE)/LiCl-based sensor with noncontact results. (**a**) Noncontact sensing of moisture on the human skin. (**b**) Results of noncontact sensing. (**c**,**d**) noncontact moisture detection for the on/off of an LED light. (**e**,**f**) Noncontact moisture detection for the on/off switching of an electric fan.

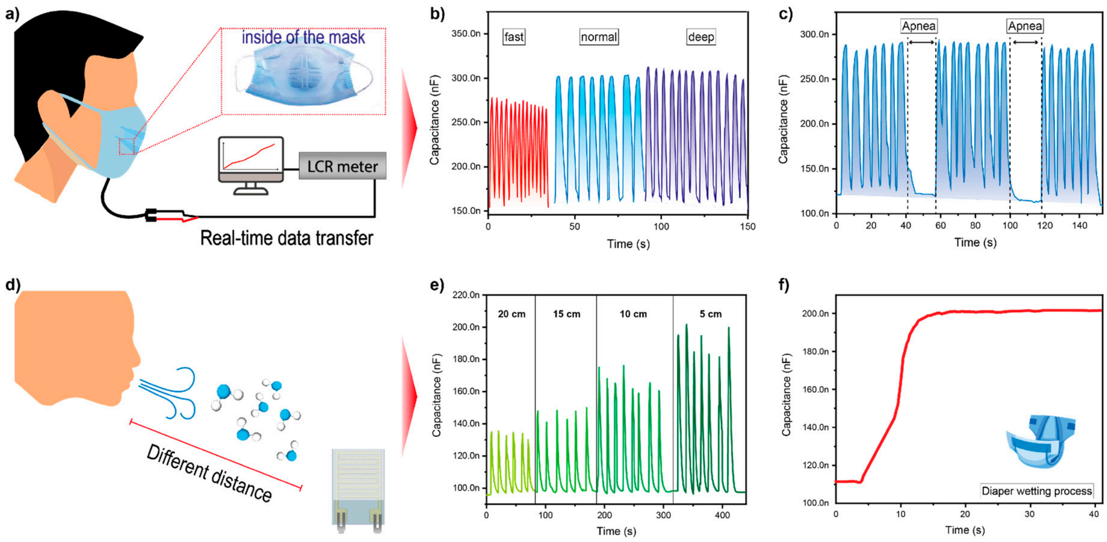

Figure 5. Real-time monitoring of the GO-doped P(VDF-TrFE)/LiCl-composite-based humidity sensor. (**a**) Schematic illustration of the experimental setup of the human respiratory monitoring. (**b**) The capacitance changes of the GO-doped P(VDF-TrFE)/LiCl-composite-based humidity sensor to deep, normal, and fast breathing. (**c**) The result of apnea and normal breathing processes. (**d**) An image of the respiration monitoring with several distances between sensors. (**e**) Capacitance variation of the distance between the sensor and the volunteer. (**f**) Diaper-wetting process.

Table 2. Humidity performance of the GO-doped P(VDF-TrFE)/LiCl-composite sensor compared with that of sensors from previous studies.

Sensing Material	Preparation Method	Measuring Range	Sensitivity	Response and Recovery Time	Ref. #/Publishing Year
SnO_2/rGO	Hydrothermal synthesis	11–97% RH	1604.89 pF/%RH	120 s	27/2016
PVDF/Graphene	Electrospinning	35–85% RH	0.0372 pF/%RH	19.8 s	25/2017
P(VDF-TrFE)/Graphene flower	Spin coating	8–98% RH	0.0558 pF/RH%	0.8 s/2.5 s	24/2021
GO-modified P(VDF-TrFE)	Electrospinning	9–90% RH	N/A	100 s	26/2022
GO-Zn1−xMnxO	Drop casting	10–90% RH	2901 pF/%RH	4.5 s and 21 s	28/2022
GO-doped P(VDF-TrFE)/LiCl	Drop casting	25–95% RH	1708.8 pF/%RH	7.8 s and 4.5 s	This work

4. Conclusions

In this study, the GO-doped P(VDF-TrFE)/LiCl-composite thin film was successfully fabricated on an IDC electrode with a simple fabrication process. Moreover, the GO-doped P(VDF-TrFE)/LiCl composite was applied in humidity-detection-based noncontact sensing and breath monitoring for the first time. The GO-doped P(VDF-TrFE)/LiCl composite formed a nanoporous structure on the IDC electrode due to the effect of LiCl. As relative humidity increased, LiCl was ionized into Li+ and Cl− on the IDC electrode. Furthermore, LiCl improved the sensitivity of the composite film, but it did not exhibit properties of noncontact sensing. Doping LiCl-contained P(VDF-TrFE) with GO increased the conductivity and reduced the response and recovery times. GO was highly sensitive to noncontact sensing, meaning that sensing properties were increased through controlling the concentration of GO. Our proposed sensor exhibited a high sensitivity of 1708.8 pF/%RH and a linearity of 0.967, with a fast response time of 7.8 s and recovery time of 4.8 s at 25% and 93% RH, respectively. Our proposed GO-doped P(VDF-TrFE)/LiCl-composite-based humidity sensor can be used in various real-time noncontact sensing applications, such as human health monitoring and noncontact electronic devices.

Supplementary Materials: The following supporting information can be downloaded at: https://www.mdpi.com/article/10.3390/chemosensors11020122/s1. Figure S1: Detailed equivalent circuit of IDC. (a) Front side of equivalent circuit with IDC electrode. (b) Top side of equivalent circuit with IDC electrode. (c) Equivalent circuit without electrode. (d) Single equivalent circuit design. Figure S2: SEM pictures. (a) P(VDF-TrFE) and (b) P(VDF-TrFE)/LiCl. Figure S3: Response and recovery time curve of P(VDF-TrFE)/LiCl. Figure S4: Circuit of the non-contact sensing device. Video S1: Comparison of non-contact sensing experiment of P(VDF-TrFE)/LiCl and GO-doped P(VDF-TrFE)/LiCl compsoite based sensors.

Author Contributions: Conceptualization and methodology, E.-S.K. and E.G.; writing—original draft preparation, data curation, software, and visualization, E.G.; writing—review and editing, E.G., E.-S.K., P.K.S., D.-N.L. and N.-Y.K.; supervision and project administration N.-Y.K. All authors have read and agreed to the published version of the manuscript.

Funding: This work was supported by the Basic Science Research Program through the National Research Foundation of Korea (NRF) funded by the Ministry of Education under Grants 2018R1A6A1A03025242, 2018R1D1A1A09083353, and 2021R1A2C1004285; in part by the Korea Ministry of Environment (MOE) Graduate School specialized in Integrated Pollution Prevention and Control Project; and a Research Grant from Kwangwoon University in 2022.

Data Availability Statement: The data presented in this study are available on request from the corresponding author. The data are not publicly available due to institutional review board restrictions.

Conflicts of Interest: The authors declare no conflict of interests.

References

1. Li, X.; Zhuang, Z.; Qi, D.; Zhao, C. High-sensitive and fast-response humidity sensor based on polymer composite nanofibers for breath monitoring and non-contact sensing. *Sens. Actuators B Chem.* **2021**, *330*, 129239. [CrossRef]
2. Pi, C.; Chen, W.; Zhou, W.; Yan, S.; Liu, Z.; Wang, C.; Guo, Q.; Qiu, J.; Yu, X.; Liu, B.; et al. Highly stable humidity sensor based on lead-free Cs3Bi2Br9 perovskite for breath monitoring. *J. Mater. Chem. C* **2021**, *9*, 11299. [CrossRef]

3. Zhang, Z.-S.; Liu, J.X.; Cheng, X.F.; He, J.H.; Li, H.; Xu, Q.F.; Li, N.J.; Chen, D.Y.; Lu, J.M. Ultrasensitive humidity sensing using one-dimensional π-d conjugated coordination polymers for breath monitoring. *Sens. Actuators B. Chem.* **2021**, *330*, 129353. [CrossRef]
4. Chen, G.; Guan, R.; Shi, M.; Dai, X.; Li, H.; Zhou, N.; Chen, D.; Mao, H. A nanoforest-based humidity sensor for respiration monitoring. *Microsyst. Nanoeng.* **2022**, *8*, 44. [CrossRef]
5. Cho, M.Y.; Kim, I.S.; Kim, S.H.; Park, C.H.; K, N.Y.; Kim, S.W.; Kim, S.H.; Oh, J.M. Unique noncontact monitoring of human respiration and sweat evaporation using a CsPb2Br5-based sensor. *ACS Appl. Mater. Interfaces* **2021**, *13*, 5602–5613. [CrossRef]
6. Sharma, P.K.; Kim, E.S.; Mishra, S.; Ganbold, E.; Seong, R.S.; Kaushik, A.K.; Kim, N.Y. Ultrasensitive and reusable graphene oxide-modified double-interdigitated capacitive (DIDC) sensing chip for detecting SARS-CoV-2. *ACS Sens.* **2021**, *6*, 3468–3476. [CrossRef]
7. Hwang, C.J.; Park, N.Y.; Kim, E.S.; Kim, M.; Kim, S.D.; Park, S.J.; Kim, N.Y.; Kim, J.H. Ultra-fast and recyclable DNA biosensor for point-of-care detection of SARS-CoV-2 (COVID-19). *Biosens. Bioelectron.* **2021**, *185*, 113177. [CrossRef]
8. Cho, M.Y.; Kim, I.S.; Kim, M.J.; Hyun, D.E.; Koo, S.M.; Sohn, H.; Kim, N.Y.; Kim, S.H.; Ko, S.H.; Oh, J.M. NaCl ionization- based moisture sensor prepared by aerosol deposition for monitoring respiratory patterns. *Sensors* **2022**, *22*, 5178. [CrossRef]
9. Kaushik, A.K.; Dhau, J.S.; Gohel, H.; Mishra, Y.K.; Kateb, B.; Kim, N.Y.; Goswami, D.Y. Electrochemical SARS-CoV-2 sensing at point-of-care and artificial intelligence for intelligent COVID-19 management. *ACS Appl. Bio. Mater.* **2020**, *11*, 7306–7325. [CrossRef]
10. Cho, M.Y.; Kim, S.H.; Kim, I.S.; Kim, E.S.; Wang, Z.J.; K, N.Y.; Kim, S.W.; Kim, S.H.; Oh, J.M. Perovskite-induced ultrasensitive and highly stable humidity sensor systems prepared by aerosol deposition at room temperature. *Adv. Func. Mater.* **2019**, *30*, 1907449. [CrossRef]
11. Yu, H.; Wang, C.; Meng, F.Y.; Liang, J.G.; Kashan, H.S.; Adhikari, K.K.; Wang, L.; Kim, E.S.; Kim, N.Y. Design and analysis of ultrafast and high- sensitivity microwave transduction humidity sensor based on belt-shaped MoO_3 nanomaterial. *Sens. Actuators B Chem.* **2020**, *304*, 127138. [CrossRef]
12. Qian, Z.; Li, T.; Sakthivelpathi, V.; Goodman, S.M.; Dichiara, A.B.; Mamishev, A.V.; Chung, J.H. Humidity response of a capacitive sensor based on auxeticity of carbon nanotube-paper composites. *Nano Express* **2020**, *3*, 025001. [CrossRef]
13. Boudaden, J.; Steinmabl, M.; Endres, H.E.; Drost, A.; Eisele, I.; Kutter, C.; Buschbaum, P.M. Polyimide-based capacitive humidity sensor. *Sensors* **2018**, *15*, 1516. [CrossRef] [PubMed]
14. Kim, J.H.; Cho, J.H.; Lee, H.M.; Hong, S.M. Capacitive humidity sensor based on carbon black/polyimide composites. *Sensors* **2021**, *21*, 1974. [CrossRef] [PubMed]
15. Qi, R.; Zhang, T.; Guan, X.; Dai, J.; Liu, S.; Zhao, H.; Fei, T. Capacitive humidity sensors based on mesoporous silica and poly(3,4-ethylenedioxythiophene) composites. *J. Colloid Interface Sci.* **2020**, *565*, 592–600. [CrossRef]
16. Tousi, M.M.; Zhang, Y.; Wan, S.; Yu, L.; Hou, C.; Yan, N.; Fink, Y.; Wang, A.; Jia, X. Scalable fabrication of highly flexible porous polymer-based capacitive humidity sensor using convergence fiber drawing. *Polymers* **2019**, *11*, 1985. [CrossRef]
17. Yang, J.; Chen, Q.; Xu, F.; Jiang, H.; Liu, W.; Zhang, X.; Jiang, Z.; Zhu, G. Epitaxy enhancement of piezoelectric properties in P(VDF-TrFE) copolymer films and applications in sensing and energy harvesting. *Adv. Electron. Mater.* **2020**, *6*, 2000578. [CrossRef]
18. Ko, Y.J.; Jin, D.W.; Kong, D.S.; Jung, J.H. Effects of humidity on the microstructure and the ferroelectric properties of sol-gel grown P(VDF-TrFE) films. *J. Korean Phys. Soc.* **2020**, *76*, 348–351. [CrossRef]
19. Kim, S.R.; Dong, Y.C.; Hossain, M.M.; Gorman, S.; Towfeeq, I.; Gajula, D.; Childress, A.; Rao, A.M.; Koley, G. Piezoresistive graphene/P(VDF-TrFE) heterostructure based highly sensitive and flexible pressure sensor. *ACS Appl. Mater. Interfaces* **2019**, *11*, 16006–16017. [CrossRef] [PubMed]
20. Dai, J.; Zhang, T.; Qi, R.; Zhao, H.; Fei, T.; Lu, G. LiCl loaded cross-linked polymer composites by click reaction for humidity sensing. *Sens. Actuators B Chem.* **2017**, *253*, 361–367. [CrossRef]
21. Fei, T.; Jiang, K.; Liu, S.; Zhang, T. Humidity sensors based on Li-loaded nanoporous polymers. *Sens. Actuators B Chem.* **2014**, *190*, 523–528. [CrossRef]
22. Feng, M.H.; Wang, W.C.; Li, X.J. LiCl-enhanced capacitive humidity-sensing properties of cadmium sulfide grown on silicon nanoporous pillar array. *J. Mater. Sci.* **2016**, *52*, 3841–3848. [CrossRef]
23. Zhuang, Z.; Li, Y.; Li, X.; Zhao, C. A novel polymer salt complex based on LiCl doped SPEEK & poly ether ketone co polyethylene glycol for humidity sensors. *IEEE Sens. J.* **2021**, *21*, 8886–8895.
24. Khan, S.A.; Saqib, M.; Rahman, M.M.; Mutee Ur Rehman, H.M.; Rahman, S.A.; Yang, Y.; Kim, S.W. A full-range flexible and printed humidity sensor based on a solution-processed P(VDF-TrFE)/graphene-flower composite. *Nanomaterials* **2021**, *11*, 1915. [CrossRef]
25. Gomez, E.S.; Martinez, R.M.; Roldan, G.R.; Rivera, D.H. A capacitive humidity sensor based on an electrospun PVDF/graphene membrane. *Sensors* **2017**, *17*, 1009.
26. Shahzad, A.; Chen, Z.; Haidry, A.A.; Yang, L.; Mehmood, A.; Khan, Z.M. GO-modified P(VDF-TrFE) fibrous membrane for humidity sensing applications in vacuum insulation panels. *Mater. Lett.* **2022**, *313*, 131773. [CrossRef]
27. Zhang, D.; Chang, H.; Li, P.; Liu, R.; Xue, Q. Fabrication and characterization of an ultrasensitive humidity sensor based on metal oxide/graphene hybrid nanocomposite. *Sens. Actuators B Chem.* **2016**, *225*, 233–240. [CrossRef]

28. Priyadharshini, B.; Valsalal, P. An improved humidity sensor with GO-Mn-doped ZnO nanocomposite and dimensional orchestration of comb electrode for effective bulk manufacturing. *Nanomaterials* **2022**, *12*, 1659. [CrossRef]
29. Liu, M.Q.; Wang, C.; Kim, N.Y. High-sensitivity and low-hysteresis porous MIM-type capacitive humidity sensor using functional polymer mixed with TiO_2 microparticles. *Sensors* **2017**, *17*, 284. [CrossRef]
30. Liang, J.G.; Kim, E.S.; Wang, C.; Cho, M.Y.; Oh, J.M.; Kim, N.Y. Thickness effects of aerosol deposited hygroscopic films on ultra-sensitive humidity sensors. *Sens. Actuat. B Chem.* **2018**, *265*, 632–643. [CrossRef]
31. Liang, J.G.; Wang, C.; Yao, Z.; Liu, M.Q.; Kim, H.K.; Oh, J.M.; Kim, N.Y. Preparation of ultrasensitive humidity-sensing films by aerosol deposition. *ACS Appl. Mater. Interfaces* **2018**, *10*, 851–863. [CrossRef]
32. Kumar, A.; Wang, C.; Meng, F.Y.; Liang, J.G.; Xie, B.F.; Zhou, Z.L.; Zhao, M.; Kim, N.Y. Aerosol deposited BaTiO3 film based interdigital capacitor and squared spiral capacitor for humidity sensing application. *Ceram. Int.* **2021**, *47*, 510–520. [CrossRef]
33. Cunha, B.B.; Greenshields, M.W.C.C.; Mamo, M.G.; Coville, N.J.; Hummelgen, I.A. A surfactant dispersed N-doped carbon sphere-poly (vinyl alcohol) composite as relative humidity sensor. *J. Mater. Sci. Mater. Electron.* **2015**, *26*, 4198–4201. [CrossRef]
34. Kim, E.S.; Liang, J.G.; Wang, C.; Cho, M.C.; Oh, J.M.; Kim, N.Y. Inter-digital capacitors with aerosol-deposited high-K dielectric layer for highest capacitance value in capacitive super-sensing applications. *Sci. Rep.* **2019**, *9*, 9680. [CrossRef]
35. Mishra, S.; Kim, E.S.; Sharma, P.K.; Wang, Z.J.; Yang, S.H.; Kaushik, A.K.; Wang, C.; Li, Y.; Kim, N.Y. Tailored biofunctionalized biosensor for the label-free sensing of prostate-specific antigen. *ACS Appl. Bio. Mater.* **2020**, *3*, 7821–7830. [CrossRef]
36. Babu Reddy, L.P.; Rajprakash, H.G.; Ravikiran, Y.T. Synthesis of α-MoO3 nanorods by sol gel synthesis and to investigate its room temperature humidity sensing properties. *AIP Conf. Proc.* **2019**, *2142*, 070022.
37. Kim, K.S.; Lee, S.; Kim, Y.I. Solvent-controlled crystalline beta-phase formation in electrospun P(VDF-TrFE) fibers for enhanced piezoelectric energy harvesting. *APL Mater.* **2020**, *8*, 071109. [CrossRef]
38. Meng, N.; Ren, X.; Santagiuliana, G.; Ventura, L.; Zhang, H.; Wu, J.; Yan, H.; Reece, M.J. Ultrahigh β-phase content poly(vinylidene fluoride) with relaxor-like ferroelectricity for high energy density capacitors. *Nat. Commun.* **2019**, *10*, 4535. [CrossRef]
39. Hu, X.; You, M.; Yi, N.; Zhang, X.; Xiang, Y. Enhanced piezoelectric coefficient of PVDF-TrFE films via in situ polarization. *Front. Energy Res.* **2021**, *9*, 321540. [CrossRef]
40. King, A.A.; Davies, B.R.; Noorbehest, N.; Newman, P.; Church, T.L.; Harris, A.T.; Razal, J.M.; Minett, A.I. A new Raman metric for the characterisation of graphene oxide and its derivatives. *Sci. Rep.* **2016**, *6*, 19491. [CrossRef]
41. Ganbold, E.; Kim, E.S.; Li, Y.; Yin, F.F.; Sharma, P.K.; Jeon, J.B.; Oh, J.M.; Lee, D.N.; Kim, N.Y. Highly Sensitive Interdigitated Capacitive Humidity Sensors Based on Sponge-Like Nanoporous PVDF/LiCl Composite for Real-Time Monitoring. *ACS App. Mater. Interfaces* **2023**, *15*, 4559–4568. [CrossRef]
42. Niu, H.; Gao, S.; Yue, W.; Li, Y.; Zhou, W.; Liu, H. Highly Morphology-Controllable and Highly Sensitive Capacitive Tactile Sensor Based on Epidermis-Dermis-Inspired Interlocked Asymmetric-Nanocone Arrays for Detection of Tiny Pressure. *Small* **2020**, *16*, 1904774. [CrossRef]